



Cite this: *Chem. Sci.*, 2024, **15**, 3495

All publication charges for this article have been paid for by the Royal Society of Chemistry

Received 8th December 2023
Accepted 26th January 2024

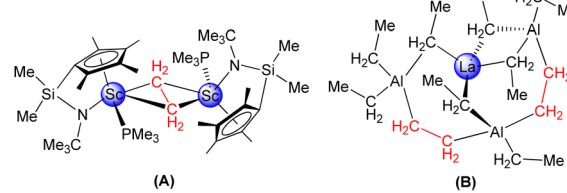
DOI: 10.1039/d3sc06599e
rsc.li/chemical-science

Introduction

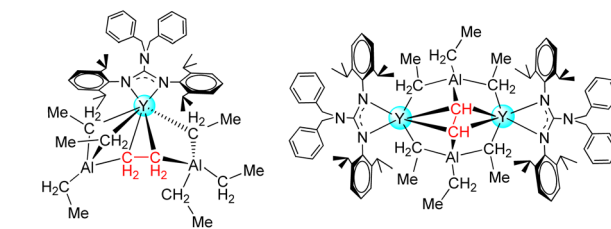
Impressive progress has been witnessed in the development of the design and synthesis of new rare-earth alkyl complexes in the last few decades owing to their high activity in a wide range of stoichiometric and catalytic reactions.^{1–3} However, studies on the alkylidene and alkylidyne complexes are limited due to the HOMO/LUMO orbital energy mismatch between the rare-earth metal ions and carbon-centered orbitals,^{4–12} among which the deprotonation of AlMe_3 and thermally induced methyl ligand degradation have been proven to be effective ways for the generation of CH_2^{2-} and CH^{3-} moieties. However, to our knowledge, compared to methyl congeners, only a few examples of rare-earth ethyl complexes and their derivatives have been isolated and structurally authenticated.^{13–16} Particularly, the rare-earth ethyl complexes engage in further degradation reactions, as shown for β -hydrogen abstraction as well as β -alkyl transfer, which are extremely limited,¹⁷ while the first ethylene complex prepared by Kaminsky's group was identified as the $\text{Zr}-\text{CH}_2\text{CH}_2-\text{Zr}$ and $\text{Zr}-\text{CH}_2\text{CH}_2-\text{Al}$ moieties generated by the reaction of Cp_2ZrCl_2 and AlEt_3 in 1974.¹⁸ Bercaw *et al.* isolated the first ethylene bridged binuclear scandium complex $\{(\text{C}_5\text{Me}_4\text{SiMe}_2\text{N}^t\text{Bu})\text{Sc}(\text{PMe}_3)\}_2(\mu\text{-C}_2\text{H}_4)$ ^{17a} (Scheme 1A). Anwander

and co-workers reported the lanthanum ethyl complex $\text{La}[(\text{Et}_3\text{Al})(\mu\text{-CH}_2\text{CH}_2)(\text{AlEt}_2)(\mu\text{-CH}_2\text{CH}_2)(\text{AlEt}_3)]$ containing two ethylene moieties^{17b} (Scheme 1B). So the study on the chemistry of rare-earth ethylene complexes is still in its infancy; we became intensely interested in the synthetic strategies and the possible reactivity of the rare-earth ethylene complexes. In addition, we are also curious about whether the rare-earth ethyne complexes can be prepared from the rare-earth ethylene complexes *via* the C–H bond activation or other pathways. To our knowledge, in contrast to the late-transition metal ethylene and ethyne complexes,^{19,20} the early-transition metal ethylene analogues are less explored,^{18,21} and no rare earth

Previous Work:



This Work:



Scheme 1 Rare-earth ethylene and ethyne complexes.

^aDepartment of Chemistry, Shanghai Key Laboratory of Molecular Catalysis and Innovative Materials, Fudan University, 2005 Songhu Road, Jiawanan Campus, Shanghai, 200438, P. R. China. E-mail: lixinzh@fudan.edu.cn

^bLPCNO, Université de Toulouse, 31077 Toulouse, France. E-mail: maron@irsamc.ups-tlse.fr

† Electronic supplementary information (ESI) available: Full experimental procedures, spectra, and analytical data. CCDC 2259604–2259609. For ESI and crystallographic data in CIF or other electronic format see DOI: <https://doi.org/10.1039/d3sc06599e>



metal ethyne complexes have been reported. With this in mind, we carried out the studies on the synthesis of rare-earth metal ethylene and ethyne complexes.

In this paper, distinctive guanidinato-based rare-earth ethylene and ethyne complexes were synthesized by controlling the molar ratio of the guanidinate dialkyl complexes²² with AlEt_3 . Moreover, the synthesis and bonding analysis (DFT) of the first rare-earth metal ethyne complex were studied.

Results and discussion

Synthesis and structural characterization

Firstly, the homoleptic rare-earth ethyl dimers $[\text{Ln}(\mu_2\text{-}\eta^1\text{-}\eta^2\text{-Et})_2]$ ($\text{Ln} = \text{Y}(\mathbf{1\text{-Y}}, 71\%), \text{Lu}(\mathbf{1\text{-Lu}}, 78\%)$) were afforded when two equivalents of AlEt_3 were added to a toluene solution of dialkyl complexes at ambient temperature (Scheme 2). In the ^1H VT NMR spectra of **1**, only one set of signals assigned to ethyl groups was observed, evidencing the rapid exchange of the ethyl-bridged and the terminal ethyl units in the solvent (Fig. S3 and S6[†]). The peak at $\delta = 0.59$ ppm for **1-Y** (0.86 ppm for **1-Lu**) is assignable to $\text{Ln}-\text{CH}_2\text{CH}_3$, and the resonance of CH_2CH_3 exhibits a peak at $\delta = 1.49$ ppm for **1-Y** (1.51 ppm for **1-Lu**). The carbon atom signals of ethyl at $\delta = 40.9, 13.1$ ppm for **1-Y** (46.8, 13.4 ppm for **1-Lu**) in the $^{13}\text{C}\{^1\text{H}\}$ NMR spectra can be considered. It is noteworthy that no hydrogen abstraction products were isolated when **1** were heated in toluene up to 70 °C for 12 h. The molecular structure of **1-Lu** is also characterized by the single-crystal X-ray diffraction (Fig. 1). The bridged ethyl units of **1-Lu** display the $\mu\text{-}\eta^1\text{:}\eta^2\text{-Et}$ bonding to the lutetium center. This coordination mode has previously been observed in the divalent Yb complex ($\text{C}_5\text{Me}_5)_2\text{Yb}(\mu\text{-}\eta^1\text{:}\eta^2\text{-Et})\text{AlEt}_3(\text{THF})^{15}$ and the trivalent Sm derivatives ($\text{C}_5\text{Me}_5)_2\text{Sm}(\text{THF})(\mu\text{-}\eta^1\text{:}\eta^2\text{-Et})\text{AlEt}_3$ (ref. 16a) and $[(\text{C}_5\text{Me}_5)_2\text{Sm}]_2[(\mu\text{-}\eta^1\text{:}\eta^2\text{-Et})_2(\mu\text{-}\eta^1\text{-Et})_2\text{Al}_4\text{Et}_6(\mu_3\text{-O})_2]$.^{16b}

According to the relevant reports of heterobimetallic Y/Al methyl complexes,²³ we might get a series of unique structural rare-earth ethyl complexes and their derivatives by controlling the amount of AlEt_3 . Thus, the treatment of $\text{LLn}(\text{CH}_2\text{C}_6\text{H}_4\text{NMe}_2\text{-}o)_2$ ($\text{Ln} = \text{Y, Lu}$) with AlEt_3 (3 equiv.) in toluene provided the heterobimetallic mixed ethyl/tetraethylaluminate complexes $\text{LLn}(\text{Et})(\mu_2\text{-}\eta^1\text{:}\eta^2\text{-Et})(\mu_2\text{-}\eta^1\text{-Et})(\text{AlEt}_2)$ ($\text{Ln} = \text{Y}(\mathbf{2\text{-Y}}, 83\%), \text{Lu}(\mathbf{2\text{-Lu}}, 90\%)$) (Scheme 3). In the NMR spectra of **2**, the distinct differences of chemical shifts of $[\text{AlEt}_4]^-$ moieties (1.30(CH_3) and 0.33(CH_2) for **2-Y**; 1.28(CH_3) and 0.53(CH_2) for **2-Lu**) and end-on-coordinated ethyl units ($\text{Ln}-\text{CH}_2\text{CH}_3$: 1.78(CH_3) and

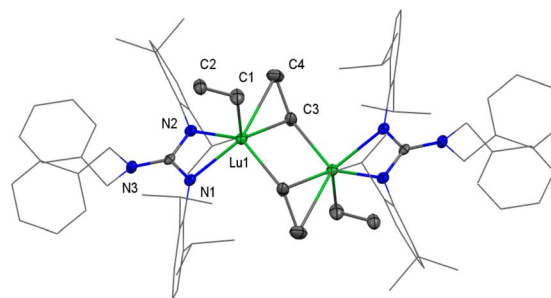
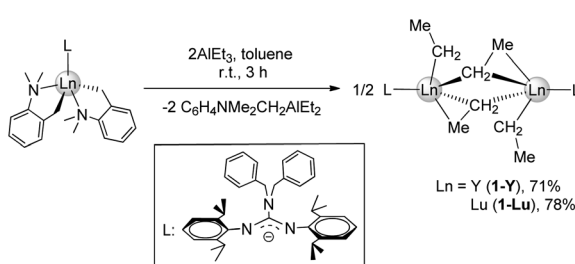


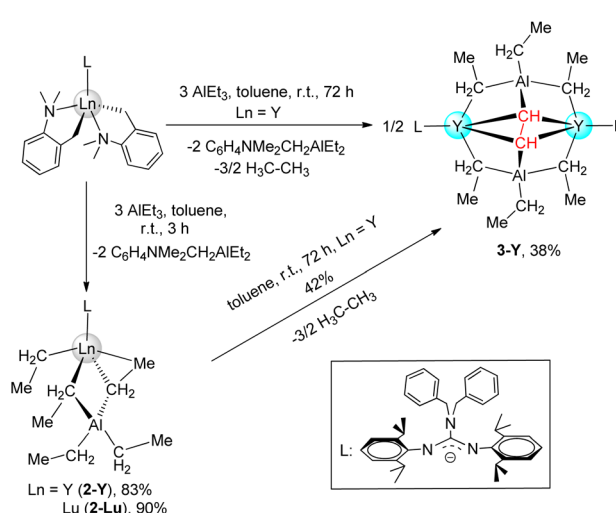
Fig. 1 Molecular structure of **1-Lu** with thermal ellipsoids at 30% probability. All hydrogen atoms are omitted for clarity. Selected bond distances (Å) and angles (°): $\text{Lu}(1)-\text{C}(1) 2.332(4)$, $\text{Lu}(1)-\text{C}(3) 2.435(4)$, $\text{Lu}(1)-\text{C}(4) 2.848(5)$, $\text{C}(1)-\text{C}(2) 1.531(6)$, $\text{C}(3)-\text{C}(4) 1.528(6)$, $\text{Lu}(1)-\text{N}(1) 2.275(3)$, $\text{Lu}(1)-\text{N}(2) 2.296(3)$; $\text{Lu}(1)-\text{C}(1)-\text{C}(2) 124.4(3)$, $\text{Lu}(1)-\text{C}(3)-\text{C}(4) 88.8(3)$, $\text{C}(1)-\text{Lu}(1)-\text{C}(3) 113.83(17)$, $\text{C}(1)-\text{Lu}(1)-\text{C}(4) 90.88(17)$.

0.85(CH_2) for **2-Y**; 1.84(CH_3) and 0.86(CH_2) for **2-Lu**) are investigated based on a comprehensive analysis of the ^{13}C DEPT-135 NMR and HMQC-NMR spectra. Additionally, the carbon atom signals of tetraethylaluminate moieties (10.8(CH_2), 10.5(CH_3) for **2-Y**; 12.8(CH_2), 10.9(CH_3) for **2-Lu**) and end-on-coordinated ethyl ligands (39.1(d, $J_{\text{YC}} = 56$ Hz, CH_2), 14.1(CH_3) for **2-Y**; 44.2(CH_2), 14.4(CH_3) for **2-Lu**) in the $^{13}\text{C}\{^1\text{H}\}$ NMR spectra can be detected. The ^{89}Y NMR spectrum of **2-Y** has a resonance at $\delta = 850.1$ ppm that is within the wide range found for the reported organometallic yttrium complexes (ESI, Fig. S11[†]).²⁴

Complexes **2** are stable under an inert atmosphere at room temperature and sparingly soluble in *n*-hexane, however, they readily dissolve in aromatic solvents. The solid-state molecular structures of **2** were determined by X-ray diffraction analysis (Fig. 2). The $\text{Ln}-\text{CH}_2\text{CH}_3$ (terminal) bond length (2.335(7) Å for **2-Y** and 2.308(8) for **2-Lu**) lies within the expected range.^{13c,14a,b} Interestingly, the bridged ethyl units of $[\text{AlEt}_4]^-$ display the $\mu\text{-}\eta^1\text{-Et}$ and $\mu\text{-}\eta^1\text{:}\eta^2\text{-Et}$ bonding to the rare-earth center, and a $\text{Ln}\cdots\text{H}_3\text{C}$ agostic interaction ($\text{Y}-\text{C}-\text{C}: 85.8(3)^\circ$; $\text{Lu}-\text{C}-\text{C}: 85.0(2)^\circ$) is likely to be present in the $\mu\text{-}\eta^1\text{:}\eta^2\text{-Et}$ bond mode.^{14d,e}



Scheme 2 Synthesis of binuclear homometallic rare-earth ethyl complexes **1**.



Scheme 3 Synthesis of heterobimetallic rare-earth ethyl complexes **2** and ethyne complex **3-Y**.



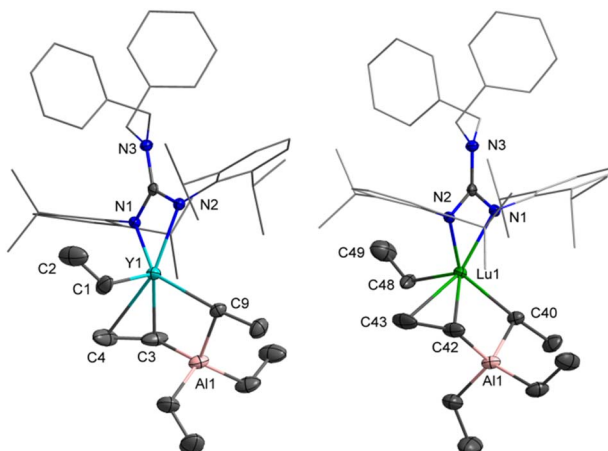


Fig. 2 Molecular structures of complexes **2-Y** (left) and **2-Lu** (right) with thermal ellipsoids at 30% probability. All hydrogen atoms are omitted for clarity. Selected bond distances (Å) and angles (°): **2-Y**: Y(1)–C(1) 2.335(7), Y(1)–C(3) 2.512(4), Y(1)–C(4) 2.838(5), Y(1)–C(9) 2.534(3), C(1)–C(2) 1.506(4), C(3)–C(4) 1.517(7), Y(1)–C(4) 2.838(5), Y(1)–Al(1) 3.043(10), Al(1)–C(3) 2.099(4), Al(1)–C(9) 2.087(3); Y(1)–C(1)–C(2) 134.4(5), Y(1)–C(3)–C(4) 85.8(3), C(1)–Y(1)–C(9) 95.9(2), C(1)–Y(1)–C(3) 110.0(2), C(3)–Y(1)–C(9) 84.88(12), C(1)–Y(1)–Al(1) 100.50(16). **2-Lu**: Lu(1)–C(40) 2.479(3), Lu(1)–C(48) 2.308(8), Lu(1)–C(42) 2.485(4), Lu(1)–C(43) 2.805(4), C(48)–C(49) 1.522(3), C(42)–C(43) 1.534(6), Lu(1)–C(43) 2.805(4), Lu(1)–Al(1) 2.988(10), Al(1)–C(40) 2.088(4), Al(1)–C(42) 2.102(4), Lu(1)–C(48)–C(49) 133.3(6), Lu(1)–C(42)–C(43) 85.0(2), C(40)–Lu(1)–C(48) 95.6(3), C(42)–Lu(1)–C(48) 109.9(3), C(40)–Lu(1)–C(42) 86.45(12), C(48)–Lu(1)–Al(1) 99.49(18).

Interestingly, the unexpected and unprecedented bridgedethyne heterobimetallic Y/Al complex $\{\text{LY}(\mu_2\text{-}\eta^1\text{-Et})_2(\text{AlEt})\}_2(\mu_4\text{-}\eta^1\text{:}\eta^1\text{:}\eta^2\text{:}\eta^2\text{-CH-CH})$ (**3-Y**) was isolated when the treatment of the yttrium dialkyl complex with AlEt_3 (3 equiv) in toluene at room temperature for 72 h was carried out. However, attempts to prepare the lutetium analogue by a similar synthetic process were unsuccessful, even at reaction temperatures up to 60 °C. Certainly, **2-Y** could be converted to **3-Y** slowly through further hydrogen abstraction reactions along with the release of ethane. The ^1H , ^{13}C { ^1H } and ^{13}C DEPT-135 NMR spectral analyses of **3-Y** in C_6D_6 are particularly informative. The one singlet signal at $\delta = 2.66$ ppm for ^1H (89.8 ppm for ^{13}C { ^1H }) is observed in the Y-bonded ethyne ligand, integrating two hydrogens, in accordance with the magnetic equivalency of the $\mu_4\text{-}\eta^1\text{:}\eta^1\text{:}\eta^2\text{:}\eta^2\text{-CH-CH}$ unit. This implies high molecular symmetry and unhindered rotation of the $\mu_4\text{-}\eta^1\text{:}\eta^1\text{:}\eta^2\text{:}\eta^2\text{-CH-CH}$ moiety in the solvent. Meanwhile, only one set of proton signals of all ethyl groups in the $[\text{Et}_3\text{Al}-\text{C}_2\text{H}_2-\text{AlEt}_3]^{4-}$ moiety is observed with a broad peak (0.33 ppm for CH_2) and a triplet (1.40 ppm for CH_3) with integral ratios of 12:18.

Red crystals of **3-Y** were crystallized from a concentrated toluene solution layered with hexane, and the X-ray structure analysis reveals a dimeric structure (Fig. 3). The Y and Al atoms are capped by the $\mu_4\text{-}\eta^1\text{:}\eta^1\text{:}\eta^2\text{:}\eta^2\text{-CH-CH}$ moiety. The characteristic feature of **3-Y** is an ethyne bridge that forms a perpendicular bisector of the Y-Y axis. This is slightly different from the osmium complex $\text{Os}_2(\text{CO})_8(\mu_2\text{-}\eta^1\text{:}\eta^1\text{-C}_2\text{H}_2)$ in which the ethyne ligand is tetra- σ bonded over a square face.^{20d} The Y–C($\mu_4\text{-CH-CH}$) bond lengths, ranging from 2.371(3) to 2.432(3) Å, are

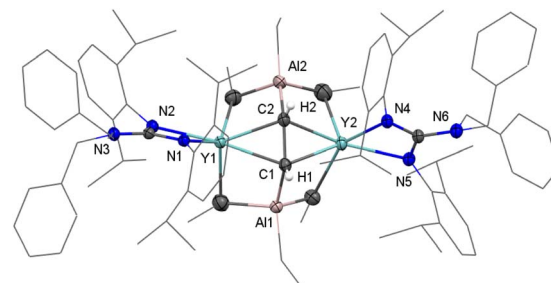
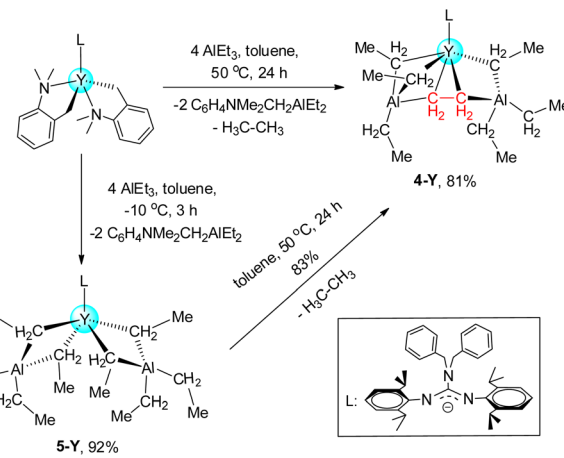


Fig. 3 Molecular structure of **3-Y** with thermal ellipsoids at 30% probability. All of the hydrogen atoms (except for H1 and H2) are omitted for clarity. Selected bond distances (Å): Y(1)–C(1) 2.432(3), Y(1)–C(2) 2.371(3), Y(2)–C(1) 2.377(3), Y(2)–C(2) 2.405(3), C(1)–C(2) 1.550(5), Al(1)–C(1) 1.976(3), Al(2)–C(2) 1.977(4); C(1)–Y(1)–C(2) 37.62(11), C(1)–C(2)–Y(1) 73.36(16), C(1)–C(2)–Al(2) 134.0(2), C(2)–C(1)–Al(1) 133.3(2).

available. Interestingly, the C–C bond length of the ethyne-bridge (1.550(5) Å) is a longish single C–C bond. This may be attributed to the generated steric hindrance of two AlEt_3 stabilization with a highly polarized Y–CHCH–Y unit, which ultimately leads to the long $\mu_4\text{-}\eta^1\text{:}\eta^1\text{:}\eta^2\text{:}\eta^2\text{-CH-CH}$ coordinated C–C bond. Until now, as far as we are aware, **3-Y** represents the first example of a well-defined rare-earth ethyne complex.

Subsequently, when four equivalents of AlEt_3 were used in the reaction with $\text{LY}(\text{CH}_2\text{C}_6\text{H}_4\text{NMe}_2\text{-}o)_2$ in toluene at room temperature, unfortunately, the isolation of major products was unsuccessful. Unexpectedly, the mononuclear heterobimetallic ethylene complex $\text{LY}(\mu_3\text{-}\eta^1\text{:}\eta^1\text{:}\eta^2\text{-C}_2\text{H}_4)[(\mu_2\text{-}\eta^1\text{-Et})(\text{AlEt}_2)]$ ($\mu_2\text{-}\eta^1\text{-Et}_2(\text{AlEt})$) (**4-Y**, 81%) was obtained while the reaction mixture was treated at 50 °C for 24 h (Scheme 4). However, we just separated out **2-Lu** as a major product when the reaction of the lutetium dialkyl complex with AlEt_3 (4 equiv) was treated under the same conditions. To get more insights into the formation process of **4-Y**, the same reaction was carried out at –10 °C for 3 h which gave a heterobimetallic Y/Al complex $\text{LY}[(\mu_2\text{-}\eta^1\text{-Et})_2(-\text{AlEt}_2)]_2$ (**5-Y**, 92%). In the NMR spectra of **5-Y**, only one set of



Scheme 4 Synthesis of heterobimetallic rare-earth ethyl complex **4-Y** and ethylene complex **5-Y**.



signals of the tetraethylaluminate moieties is observed in C_6D_6 at room temperature^{13d} (Fig. S23–S24†), which is also similar to the $[\text{AlMe}_4]^-$ ligands.^{7b,23} Crucially, **5-Y** could be transformed into **4-Y** in toluene at 50 °C for 24 h with the release of ethane through the β -hydrogen abstraction reaction²⁵ (Fig. S25†). It is well established that **5-Y** is a crucial intermediate in the formation of **4-Y**. A broad singlet at $\delta = 0.81$ ppm in the ^1H NMR spectrum of **4-Y** is assignable to the ethylene moiety of the type $\text{Y}-\text{CH}_2\text{CH}_2-\text{Y}$, integrating to four hydrogens, which is comparable to the ethylene resonance found for the lanthanum complex $(\text{AlEt}_4)\text{La}\{(\mu\text{-Et})(\text{AlEt}_2)\}_2(\mu\text{-C}_2\text{H}_4)$ ^{17b} (^1H NMR: 0.81 ppm in C_6D_6). However, these signals shifted markedly compared to the ethyne resonance found for **3-Y**, verifying the differences in the core structural units. In the $^{13}\text{C}\{^1\text{H}\}$ NMR spectrum, the $\delta = 13.3$ ($J_{\text{YC}} = 7$ Hz) ppm is also observed as the carbon signal of the $\text{Y}-\text{CH}_2\text{CH}_2-\text{Y}$ moiety. Compared to **2-Y**, the chemical shift of the ^{89}Y of **4-Y** (326.4 ppm, Fig. S22†) toward the higher field might be attributed to the coordination of AlEt_3 and increased electronegativity of the $\mu_3\text{-}\eta^1\text{-}\eta^1\text{-}\eta^2\text{-C}_2\text{H}_4$ moiety.²⁴

4-Y was further characterized by X-ray diffraction analysis (Fig. 4). From structural parameters, the $\text{Y}-\text{C}(\mu_2\text{-C}_2\text{H}_4)$ distances (2.475(9) and 2.689(9) Å) are slightly longer than in $\{(\text{C}_5\text{Me}_4\text{-SiMe}_2\text{N}^t\text{Bu})\text{Sc}(\text{PMe}_3)\}_2(\mu\text{-C}_2\text{H}_4)$ (2.320(9) and 2.357(9) Å) when the difference between metallic radii is considered. Besides, the C–C bond length of ethylene-bridged (1.533(13) Å) is longer than the bond length observed in $\{(\text{C}_5\text{Me}_4\text{SiMe}_2\text{N}^t\text{Bu})\text{Sc}(\text{PMe}_3)\}_2(\mu\text{-}\eta^2\text{-}\eta^2\text{-C}_2\text{H}_4)$ (1.433 (12) Å), and which is unlikely to the C=C distance in free ethylene (1.34 Å)²⁶ while the length approaches a value typical of a carbon–carbon single bond, such as 1.522(2) Å in ethane.²⁷ To our knowledge, **4-Y** is the only well-defined non-Cp rare-earth ethylene complex. The molecular structure of **5-Y** is also characterized by X-ray diffraction analysis (Fig. 5). The bridged ethyl units of $[\text{AlEt}_4]^-$ only display the $\mu\text{-}\eta^1\text{-ethyl}$ bonding to the yttrium center, similar to previous Ln/Al heterobimetallic ethyl complexes containing $[\text{AlEt}_4]^-$ moieties.^{13a,c,e,g}

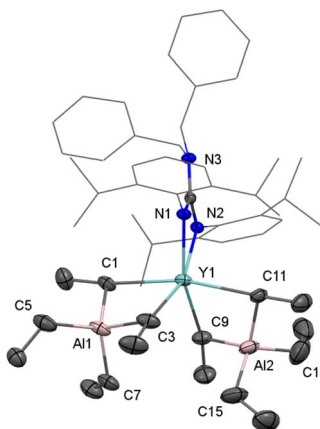


Fig. 5 Molecular structure of complex **5-Y** with thermal ellipsoids at 30% probability except for the $2,6-(^1\text{Pr})_2\text{C}_6\text{H}_3$ groups and benzyl groups in the guanidinate ligand. All hydrogen atoms are omitted for clarity. Selected bond distances (Å) and angles (°): $\text{Y}(1)-\text{C}(1)$ 2.619(4), $\text{Y}(1)-\text{C}(3)$ 2.572(4), $\text{Y}(1)-\text{C}(9)$ 2.564(3), $\text{Y}(1)-\text{C}(11)$ 2.622(8), $\text{Y}(1)-\text{N}(1)$ 2.336(2), $\text{Y}(1)-\text{N}(2)$ 2.299(2), $\text{Al}(1)-\text{C}(5)$ 2.008(5), $\text{Al}(1)-\text{C}(7)$ 2.004(4), $\text{Al}(2)-\text{C}(13)$ 1.956(6), $\text{Al}(2)-\text{C}(15)$ 2.024(5); $\text{C}(1)-\text{Y}(1)-\text{C}(3)$ 78.12(12), $\text{C}(1)-\text{Y}(1)-\text{C}(9)$ 89.45(12), $\text{C}(1)-\text{Y}(1)-\text{C}(11)$ 165.9(2), $\text{Y}(1)-\text{C}(1)-\text{Al}(1)$ 85.17(13), $\text{Y}(1)-\text{C}(9)-\text{Al}(2)$ 83.92(12).

DFT calculations

The formation of **1-Y**, **2-Y**, and **3-Y** was investigated computationally at the DFT level (B3PW91 functional) including solvent and dispersion corrections (Fig. 6). The reaction begins by the electrophilic attack of the aluminum to the benzylic carbon, which occurs with almost no barrier (2.7 kcal mol⁻¹) to form a stable intermediate (**Int2**). **Int2** isomerizes in order to have an ethyl group in the bridging position between Y and Al. This isomerization allows the formation of **Int3** with an energy cost of 14.3 kcal mol⁻¹. This isomerization allows a kinetically facile Al-Et bond breaking (barrier of 0.6 kcal mol⁻¹ from **Int3**, 14.9 kcal mol⁻¹ from **Int2**). Following the intrinsic reaction coordinate, it yields an yttrium aminobenzyl/ethyl complex **Int5**, which further reacts in a similar fashion with a second triethylaluminium molecule. The same sequence of reaction as described previously allows the formation of a quite unstable monomeric guanidinato-yttrium diethyl complex (**Int8**), that can either dimerize to form **1-Y**, which is thermodynamically favored by 69.1 kcal mol⁻¹ or can further react with a third molecule of triethylaluminium to yield **2-Y**, which is also thermodynamically favorable (−53.1 kcal mol⁻¹).

Interestingly, **2-Y** can undergo a C–H activation reaction with a barrier of 26.3 kcal mol⁻¹ to yield **Int9**, which dimerizes to form the most stable complex **3-Y** accompanying C–C bond cleavage (Me–CH) and new C–C bond formation (CH–CH) (−90.2 kcal mol⁻¹). To gain more insights into the bonding properties of the yttrium ethyne complex, DFT calculations on **3-Y** were carried out. Scrutinizing the molecular orbitals indicates that the HOMO-7 and HOMO-4 are Y–C σ bonding interactions (Fig. 7). The bonding situation is further confirmed by the Natural bonding orbital (NBO) analysis and the Wiberg bond indexes (WBIs). The geometry optimization (B3PW91) of **3-Y** revealed structural parameters in agreement with their experimental counterparts: the C_1-C_2 (1.531 Å) distance

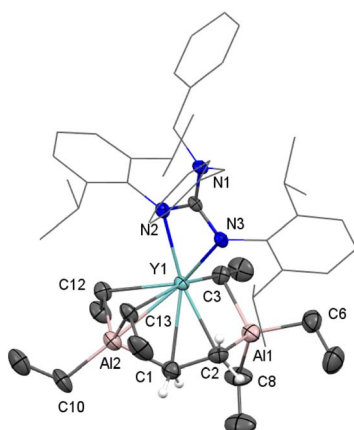


Fig. 4 Molecular structure of **4-Y** with thermal ellipsoids at 30% probability. All of the hydrogen atoms (except for H1 and H2) are omitted for clarity. Selected bond distances (Å) and angles (°): $\text{Y}(1)-\text{C}(1)$ 2.689(9), $\text{Y}(1)-\text{C}(2)$ 2.475(9), $\text{C}(1)-\text{C}(2)$ 1.533(13), $\text{Al}(1)-\text{C}(2)$ 2.047(10), $\text{Al}(2)-\text{C}(1)$ 2.071(10); $\text{C}(1)-\text{Y}(1)-\text{C}(2)$ 34.2(3), $\text{Y}(1)-\text{C}(1)-\text{C}(2)$ 65.2(4), $\text{Y}(1)-\text{C}(2)-\text{C}(1)$ 80.6(5), $\text{Y}(1)-\text{C}(1)-\text{Al}(2)$ 70.3(3), $\text{Y}(1)-\text{C}(2)-\text{Al}(1)$ 84.4(3).



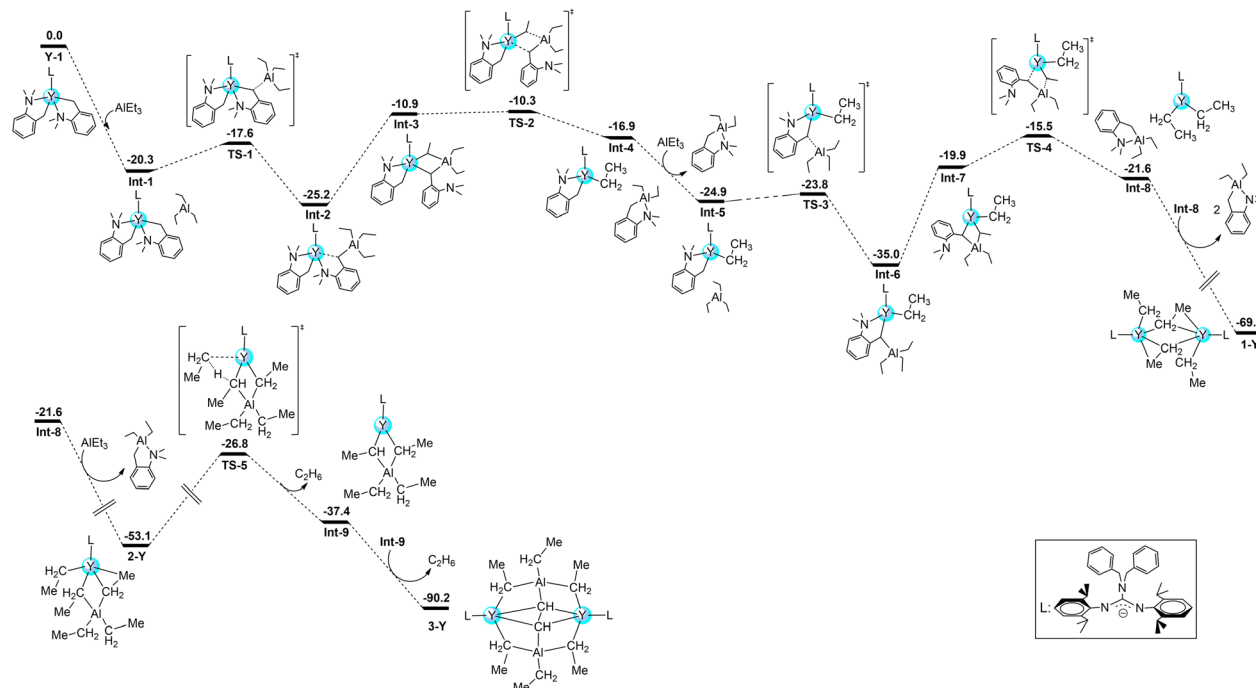


Fig. 6 Computed enthalpy pathway at the DFT level for the formation of **1-Y**, **2-Y**, and **3-Y** at room temperature. Energy is given in kcal mol^{-1} .

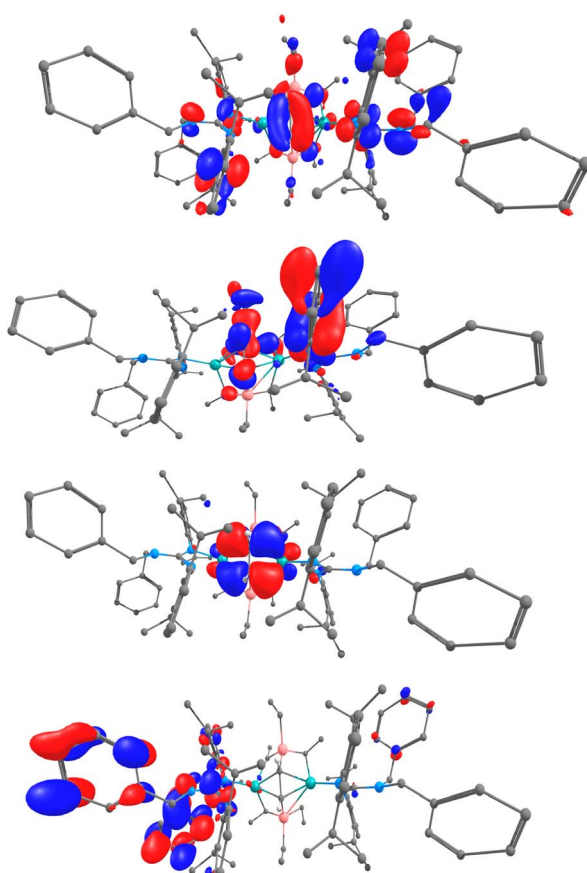


Fig. 7 DFT computed MOs for the yttrium ethyne complex **3-Y**: (a) HOMO-7, (b) HOMO-4, (c) HOMO, (d) LUMO. Atom color code: green, yttrium; blue, nitrogen; gray, carbon; and white, hydrogen.

resembled the observed X-ray distances of $1.550(5)$ Å. Indeed, the Wiberg bond index (WBI) is 1.02 for the C1-C2, in line with the lack of π interaction in the ethyne unit. The Y-C WBI values are 0.36, 0.39, 0.41, and 0.42 respectively, further corroborating the single bond character of the C1-C2 interaction. The polarized nature of the bonds is further demonstrated and the charges carried by the ethyne carbon are -1.40 and -1.41 , whereas those of the ethyne hydrogen are $+0.29$ and $+0.29$.

Conclusions

In summary, we have successfully isolated and structurally characterized guanidinato-stabilized homo-metallic and hetero-bimetallic rare-earth ethyl complexes through transmetalation reactions. To our excitement, not only the first example of a non-Cp rare-earth ethylene complex through the β -H abstraction was isolated successfully, but also a unique well-defined rare-earth ethyne complex was obtained by the α -H abstraction and C-C σ bond metathesis process based on the mechanism studies by DFT calculations. Studies on the reaction chemistry of these hitherto unexplored $\mu_2\text{-CH}_2\text{CH}_2$ and $\mu_4\text{-CHCH}$ moieties are underway.

Data availability

The data that support the findings of this study are available in the ESI[†] of this article.

Author contributions

Mr Wen Jiang carried out the experiments, crystal analyses and manuscript writing. Dr Thayalan Rajeshkumar and Prof.



Laurent Maron are responsible for the DFT calculation. Dr Yuejian Lin helped Wen Jiang in crystal analyses. Miss. Guo Mengyue assisted Mr Jiangwen to synthesize the raw materials. Prof. Zhang Lixin designed the experiments and revised this paper.

Conflicts of interest

The authors declare no conflict of interest.

Acknowledgements

This work was supported by the National Natural Science Foundation of China (grant nos 21871052). We are grateful to Prof. Xigeng Zhou and Prof Huadong Wang at Fudan University for helpful discussion. The authors acknowledge the HPCs CALcul en Midi-Pyrénées (CALMIP-EOS grant 1415).

Notes and references

- (a) M. Zimmermann and R. Anwander, *Chem. Rev.*, 2010, **110**, 6194–6259; (b) F. T. Edelmann, *Chem. Soc. Rev.*, 2012, **41**, 7657–7672; (c) A. A. Trifonov and D. M. Lyubov, *Coord. Chem. Rev.*, 2017, **340**, 10–61.
- (a) Z. Hou and Y. Wakatsuki, *Coord. Chem. Rev.*, 2002, **231**, 1–22; (b) J. Gromada, J. F. Carpentier and A. Mortreux, *Coord. Chem. Rev.*, 2004, **248**, 397–410; (c) M. Nishiura and Z. Hou, *Nat. Chem.*, 2010, **2**, 257–268; (d) M. Nishiura, F. Guo and Z. Hou, *Acc. Chem. Res.*, 2015, **48**, 2209–2220.
- (a) S. Hong and T. J. Marks, *Acc. Chem. Res.*, 2004, **37**, 673–686; (b) T. E. Muller, K. C. Hultsch, M. Yus, F. Foubelo and M. Tada, *Chem. Rev.*, 2008, **108**, 3795–3892; (c) D. M. Lyubov and A. A. Trifonov, *Inorg. Chem. Front.*, 2021, **8**, 2965–2986; (d) F. Ortu, *Chem. Rev.*, 2022, **122**, 6040–6116.
- (a) K. Aparna, M. Ferguson and R. G. Cavell, *J. Am. Chem. Soc.*, 2000, **122**, 726–727; (b) D. P. Mills, L. Soutar, W. Lewis, A. J. Blake and S. T. Liddle, *J. Am. Chem. Soc.*, 2010, **132**, 14379–14381; (c) M. Fustier, X. F. Le Goff, P. Le Floch and N. Mézailles, *J. Am. Chem. Soc.*, 2010, **132**, 13108–13110; (d) S. T. Liddle, D. P. Mills and A. J. Woole, *Chem. Soc. Rev.*, 2011, **40**, 2164–2176; (e) M. Fustier, X. F. Le Goff, M. Lutz, J. C. Slootweg and N. Mézailles, *Organometallics*, 2015, **34**, 63–72.
- H. M. Dietrich, K. W. Törnroos and R. Anwander, *J. Am. Chem. Soc.*, 2006, **128**, 9298–9299.
- (a) M. Zimmermann, D. Rauschmaier, K. Eichele, K. W. Törnroos and R. Anwander, *Chem. Commun.*, 2010, **46**, 5346–5348; (b) J. Hong, L. Zhang, X. Yu, M. Li, Z. Zhang, P. Zheng, M. Nishiura, Z. Hou and X. Zhou, *Chem.-Eur. J.*, 2011, **17**, 2130–2137; (c) J. Hong, L. Zhang, K. Wang, Y. Zhang, L. Weng and X. Zhou, *Chem.-Eur. J.*, 2013, **19**, 7865–7873; (d) K. Wang, G. Luo, J. Hong, X. Zhou, H. Weng, Y. Luo and L. Zhang, *Angew. Chem., Int. Ed.*, 2014, **53**, 1053–1056; (e) J. Hong, Z. Li, Z. Chen, L. Weng, X. Zhou and L. Zhang, *Dalton Trans.*, 2016, **45**, 6641–6649; (f) H. Tian, J. Hong, K. Wang, I. Rosal, L. Maron, X. Zhou and L. Zhang, *J. Am. Chem. Soc.*, 2018, **140**, 102–105; (g) J. Hong, H. Tian, L. Zhang, X. Zhou, I. del Rosal, L. Weng and L. Maron, *Angew. Chem., Int. Ed.*, 2018, **57**, 1062–1067; (h) C. O. Hollfelder, L. N. Jende, H. M. Dietrich, K. Eichele, C. Maichle-Mössmer and R. Anwander, *Chem.-Eur. J.*, 2019, **25**, 7298–7302; (i) C. O. Hollfelder, M. Zimmermann, C. Spiridopoulos, D. Werner, K. W. Törnroos, C. Maichle-Mössmer and R. Anwander, *Molecules*, 2019, **24**, 3703–3730; (j) D. A. Buschmann, L. Schumacher and R. Anwander, *Chem. Commun.*, 2022, **58**, 9132–9135.
- (a) M. Zimmermann, J. Takats, G. Kiel, K. W. Törnroos and R. Anwander, *Chem. Commun.*, 2008, 612–614; (b) J. Scott, H. J. Fan, B. F. Wicker, A. R. Fout, M. H. Baik and D. J. Mindiola, *J. Am. Chem. Soc.*, 2008, **130**, 14438–14439; (c) R. Litlabø, M. Zimmermann, K. Saliu, J. Takats, K. W. Törnroos and R. Anwander, *Angew. Chem., Int. Ed.*, 2008, **47**, 9560–9564; (d) A. Venugopal, I. Kamps, D. Bojer, R. J. F. Berger, A. Mix, A. Willner, B. Neumann, H.-G. Stammle and N. W. Mitzel, *Dalton Trans.*, 2009, 5755–5765; (e) I. Korobkov and S. Gambarotta, *Organometallics*, 2009, **28**, 5560–5567; (f) W. Huang, C. T. Carver and P. L. Diaconescu, *Inorg. Chem.*, 2011, **50**, 978–984; (g) D. Barisic, D. Diether, C. Maichle-Mössmer and R. Anwander, *J. Am. Chem. Soc.*, 2019, **141**, 13931–13940; (h) P. Zatsepin, E. Lee, J. Gu, M. R. Gau, P. J. Carroll, M. Baik and D. J. Mindiola, *J. Am. Chem. Soc.*, 2020, **142**, 10143–10152; (i) T. E. Rieser, R. Thim-Spöring, D. Schädle, P. Sirsch, R. Litlabø, K. W. Törnroos, C. Maichle-Mössmer and R. Anwander, *J. Am. Chem. Soc.*, 2022, **144**, 4102–4113.
- (a) W. Zhang, Z. Wang, M. Nishiura, Z. Xi and Z. Hou, *J. Am. Chem. Soc.*, 2011, **133**, 5712–5715; (b) T. Li, M. Nishiura, J. Cheng, Y. Li and Z. Hou, *Chem.-Eur. J.*, 2012, **18**, 15079–15085.
- (a) S. Li, M. Wang, B. Liu, L. Li, J. Cheng, C. Wu, D. Liu, J. Liu and D. Cui, *Chem.-Eur. J.*, 2014, **20**, 15493–15498; (b) T. Shima, T. Yanagi and Z. Hou, *New J. Chem.*, 2015, **39**, 7608–7616; (c) J. Zhou, T. Li, L. Maron, X. Leng and Y. Chen, *Organometallics*, 2015, **34**, 470–476; (d) T. Li, G. Zhang, J. Guo, S. Wang, X. Leng and Y. Chen, *Organometallics*, 2016, **35**, 1565–1572; (e) F. Yan, S. Li, L. Li, W. Zhang, D. Cui, M. Wang and Y. Dou, *Eur. J. Inorg. Chem.*, 2019, **17**, 2277–2283.
- (a) D. J. Mindiola and J. Scott, *Nat. Chem.*, 2011, **3**, 15–17; (b) C. Wang, J. Zhou, X. Zhao, L. Maron, X. Leng and Y. Chen, *Chem.-Eur. J.*, 2016, **22**, 1258–1261; (c) W. Mao, L. Xiang, L. Maron, X. Leng and Y. Chen, *J. Am. Chem. Soc.*, 2017, **139**, 17759–17762; (d) W. Mao, L. Xiang, C. A. Lamsfus, L. Maron, X. Leng and Y. Chen, *J. Am. Chem. Soc.*, 2017, **139**, 1081–1084; (e) W. Mao, L. Xiang, C. A. Lamsfus, L. Maron, X. Leng and Y. Chen, *Chin. J. Chem.*, 2018, **36**, 904–908; (f) C. Wang, L. Xiang, Y. Yang, J. Fang, L. Maron, X. Leng and Y. Chen, *Chem.-Eur. J.*, 2018, **24**, 5637–5643; (g) C. Wang, W. Mao, L. Xiang, Y. Yang, J. Fang, L. Maron, X. Leng and Y. Chen, *Chem.-Eur. J.*, 2018, **24**, 13903–13917; (h) W. Mao, Y. Wang, L. Xiang, Q. Peng, X. Leng and Y. Chen, *Chem.-Eur. J.*, 2019, **25**, 10304–10308.



11 (a) W. Ma, C. Yu, Y. Chi, T. Chen, L. Wang, J. Yin, B. Wei, L. Xu, W. Zhang and Z. Xi, *Chem. Sci.*, 2017, **8**, 6852–6856; (b) Y. Zheng, C. Cao, W. Ma, T. Chen, B. Wu, C. Yu, Z. Huang, J. Yin, H. Hu, J. Li, W. Zhang and Z. Xi, *J. Am. Chem. Soc.*, 2020, **142**, 10705–10714.

12 (a) H. M. Dietrich, H. Grove, K. W. Törnroos and R. Anwander, *J. Am. Chem. Soc.*, 2006, **128**, 1458–1459; (b) L. C. H. Gerber, E. Le Roux, K. W. Törnroos and R. Anwander, *Chem.-Eur. J.*, 2008, **14**, 9555–9564; (c) D. Bojer, A. Venugopal, B. Neumann, H.-G. Stammmer and N. W. Mitzel, *Angew. Chem., Int. Ed.*, 2010, **49**, 2611–2614; (d) D. Bojer, B. Neumann, H.-G. Stammmer and N. W. Mitzel, *Chem.-Eur. J.*, 2011, **17**, 6239–6247; (e) D. Bojer, B. Neumann, H.-G. Stammmer and N. W. Mitzel, *Eur. J. Inorg. Chem.*, 2011, 3791–3796; (f) P. Deng, X. Shi, X. Gong and J. Cheng, *Chem. Commun.*, 2021, **57**, 6436–6439; (g) W. Jiang, F. Kong, I. Rosal, M. Li, K. Wang, L. Maron and L. Zhang, *Chem. Sci.*, 2023, **14**, 9154–9160.

13 (a) W. J. Evans, L. R. Chamberlain and J. W. Ziller, *J. Am. Chem. Soc.*, 1987, **109**, 7209–7211; (b) D. Stern, M. Sabat and T. J. Marks, *J. Am. Chem. Soc.*, 1990, **112**, 9558–9575; (c) M. G. Klimpel, J. Eppinger, P. Sirsch, W. Scherer and R. Anwander, *Organometallics*, 2002, **21**, 4021–4023; (d) A. Fischbach, M. G. Klimpel, M. Widenmeyer, E. Herdtweck, W. Scherer and R. Anwander, *Angew. Chem., Int. Ed.*, 2004, **43**, 2234–2239; (e) M. G. Schrems, H. M. Dietrich, K. W. Törnroos and R. Anwander, *Chem. Commun.*, 2005, 5922–5924; (f) A. Fischbach, F. Perdih, E. Herdtweck and R. Anwander, *Organometallics*, 2006, **25**, 1626–1642; (g) H. Sommerfeldt, C. Meermann, M. G. Schrems, K. W. Törnroos, N. Frøystein, R. J. Miller, E. Scheidt, W. Scherer and R. Anwander, *Dalton Trans.*, 2008, 1899–1907.

14 (a) M. D. Fryzuk, G. Giesbrecht and S. J. Rettig, *Organometallics*, 1996, **15**, 3329–3336; (b) T. I. Gountchev and T. D. Tilley, *Organometallics*, 1999, **18**, 2896–2905; (c) P. G. Hayes, W. E. Piers, L. W. M. Lee, L. K. Knight, M. Parvez, M. R. J. Elsegood and W. Clegg, *Organometallics*, 2001, **20**, 2533–2544; (d) M. R. MacDonald, R. R. Langeslay, J. W. Ziller and W. J. Evans, *J. Am. Chem. Soc.*, 2015, **137**, 14716–14725; (e) D. B. Culver, W. Huynh, H. Tafazolian, T. C. Ong and M. P. Conley, *Angew. Chem., Int. Ed.*, 2018, **57**, 9520–9523.

15 H. Yamamoto, H. Yasuda, K. Yokota, A. Nakamura, Y. Kai and N. Kasai, *Chem. Lett.*, 1988, 1963–1966.

16 (a) W. J. Evans, T. M. Champagne, D. G. Giarikos and J. W. Ziller, *Organometallics*, 2005, **24**, 570–579; (b) W. J. Evans, T. M. Champagne and J. W. Ziller, *Organometallics*, 2005, **24**, 4882–4885.

17 (a) P. J. Shapiro, W. P. Schaefer, J. A. Labinger, J. E. Bercaw and W. D. Cotter, *J. Am. Chem. Soc.*, 1994, **116**, 4623–4640; (b) H. M. Dietrich, K. W. Törnroos and R. Anwander, *Angew. Chem., Int. Ed.*, 2011, **50**, 12089–12093.

18 (a) W. Kaminsky, J. Kopf and G. Thirase, *Adv. Cycloaddit.*, 1974, 1531–1533; (b) W. Kaminsky and H. Sinn, *Adv. Cycloaddit.*, 1975, 424–437; (c) W. Kaminsky and H. Sinn, *Adv. Cycloaddit.*, 1975, 438–448; (d) W. Kaminsky, J. Kopf, H. Sinn and H. J. Vollmer, *Angew. Chem., Int. Ed. Engl.*, 1976, **15**, 629–630.

19 (a) L. H. Shultz, D. J. Tempel and M. Brookhart, *J. Am. Chem. Soc.*, 2001, **123**, 11539–11555; (b) X. Dai and T. H. Warren, *Chem. Commun.*, 2001, 1998–1999; (c) H. V. Rasika Dias, M. Fianchini, T. R. Cundari and C. F. Campana, *Angew. Chem., Int. Ed.*, 2008, **47**, 556–559; (d) J. Wolf, K. Thommes, O. Briel, R. Scopelliti and K. Severin, *Organometallics*, 2008, **27**, 4464–4474; (e) H. V. Rasika Dias and J. Wu, *Eur. J. Inorg. Chem.*, 2008, 509–522; (f) Y. Segawa, M. Yamashita and K. Nozaki, *Organometallics*, 2009, **28**, 6234–6242; (g) P. Ebrahimpour, M. F. Haddow and D. F. Wass, *Inorg. Chem.*, 2013, **52**, 3765–3771; (h) M. Navarro, M. G. Alférez, M. de Sousa, J. Miranda-Pizarro and J. Campos, *ACS Catal.*, 2022, **12**, 4227–4241; (i) M. Maekawa, T. Hayashi, K. Sugimoto, T. Okubo and T. Kuroda-Sowa, *Dalton Trans.*, 2023, **52**, 14941–14948.

20 (a) G. Gervasio, R. Rossetti and P. L. Stanghellini, *Organometallics*, 1985, **4**, 1612–1619; (b) S. F. Parker, P. H. Dallin, B. T. Keiller, C. E. Anson and U. A. Jayasooriya, *Phys. Chem. Chem. Phys.*, 1999, **1**, 2589–2592; (c) G. Kiel, Z. Zhang, J. Takats and R. B. Jordan, *Organometallics*, 2000, **19**, 2766–2776; (d) C. E. Anson, N. Sheppard, R. Pearman, J. R. Moss, P. Stofsel, S. Koch and J. R. Norton, *Phys. Chem. Chem. Phys.*, 2004, **6**, 1070–1076; (e) J. A. Platts, G. J. S. Evans, M. P. Coogan and J. Overgaard, *Inorg. Chem.*, 2007, **46**, 6291–6298.

21 (a) E. Durgun, S. Ciraci, W. Zhou and T. Yildirim, *Phys. Rev. Lett.*, 2006, **97**, 226102; (b) N. Wadnerkar, V. Kalamse and A. Chaudhari, *RSC Adv.*, 2012, **2**, 8497–8501.

22 F. Kong, M. Li, X. Zhou and L. Zhang, *RSC Adv.*, 2017, **7**, 29752–29761.

23 (a) N. Dettenrieder, H. M. Dietrich, C. Schädle, C. Maichle-Mössmer, K. W. Törnroos and R. Anwander, *Angew. Chem., Int. Ed.*, 2012, **51**, 4461–4465; (b) W. Rong, M. Wang, S. Li, J. Cheng, D. Liu and D. Cui, *Organometallics*, 2018, **37**, 971–978.

24 (a) C. J. Schaverien, *Organometallics*, 1994, **13**, 69–82; (b) R. E. White and T. P. Hanusa, *Organometallics*, 2006, **25**, 5621–5630; (c) C. Schädle, A. Fischbach, E. Herdtweck, K. W. Törnroos and R. Anwander, *Chem.-Eur. J.*, 2013, **19**, 16334–16341; (d) L. Lätsch, E. Lam and C. Copéret, *Chem. Sci.*, 2020, **11**, 6724–6735.

25 P. Bertus, *Organometallics*, 2019, **38**, 4171–4182.

26 F. A. Cotton, E. V. Dikarev, M. A. Petrukhina and R. E. Taylor, *J. Am. Chem. Soc.*, 2001, **123**, 5831–5832.

27 M. D. Harmony, Chapter 1 Molecular Structure Determination from Spectroscopic Data Using Scaled Moments of Inertia, in *Equilibrium Structural Parameters*, ed. J. R. Durig, Elsevier, Oxford, U.K., Vibra-tional Spectra and Structure, 1999, vol. 24, pp. 1–83.

